would find for $g^4(T/\theta)^5 \ll \Gamma/E_F$ that

$$\Delta_T \sim g^4(T/\theta)^5 \ln(\rho_0/\rho_T{}^{\text{pure}}). \quad (19)$$

For $T/\theta \ll 1$ it is possible (but not likely) for expression (19) to be greater than expression (18) and still have $g^2(T/\theta)^3 \ll (\lambda k_F)^{-1} \sim \Gamma/E_F$, as required in order that λ be determined essentially by the electron-impurity interactions. The low-temperature resistivity of dilute alloys of Au has been studied by Damon, Mathur, and Klemens[10]; it appears possible to express their results in the form of Eq. (19). In any event, our mechanism allows the possibility of understanding the different behavior observed in Au and Al in terms of differences in the Fermi surface of these metals, whereas the mechanism of Mills and Campbell, Caplin, and Rizzuto does not.

We might also note that our analysis in the cylindrical case [and Eq. (19) in the spherical case] would also apply if electron-boundary, rather than electron-impurity, interactions were dominant.[11]

We have neglected the effects of phonon-impurity scattering, umklapp processes, the fact that the crystal is clamped, etc. These are not inconsequential, and we hope to present a detailed analysis in a future paper.

The author wishes to thank J. E. Neighbor and R. I. Boughton both for bringing this question to the author's attention and for numerous valuable discussions.

[1]A. D. Caplin and C. Rizzuto, J. Phys. C: Proc. Phys. Soc., London 3, L117 (1970).

[2]I. A. Campbell, A. D. Caplin, and C. Rizzuto, Phys. Rev. Lett. 26, 239 (1971).

[3]D. L. Mills, Phys. Rev. Lett. 26, 242 (1971).

[4]Mills, Ref. 3, does not distinguish between a true second order process and the product of two first order ones (which are automatically included in the Boltzmann equation), but we shall overlook this.

[5]This is because the phonon vertices may be placed in all possible positions along the electron lines (e.g., they may appear as vertex corrections to the impurity scattering as well as in the collision terms considered by Mills).

[6]T. Holstein, Ann. Phys. (New York) 29, 410 (1964).

[7]T. Neal, Phys. Rev. 169, 508 (1968).

[8]J. S. Langer and T. Neal, Phys. Rev. Lett. 16, 984 (1966).

[9]We may include the ladder sum over *all* numbers of rungs [Fig. 2(a) corresponding to a single rung] for both the cylindrical and spherical cases; the resulting expressions for Δ_T would be essentially unchanged from the values given in Eqs. (16) and (18). [Compare Eqs. (4.32) and (5.20) of Ref. 7.]

[10]D. H. Damon, M. P. Mathur, and P. G. Klemens, Phys. Rev. 176, 876 (1968).

[11]In this case additional contritutions to Δ_T similar to Eqs. (16) and (18) may arise as from the "size-effect" contribution to the resistivity, depending on the nature of the Fermi surface, as noted by J. E. Neighbor and R. I. Boughton, to be published.

Optical Phonon Lifetime Measured Directly with Picosecond Pulses

R. R. Alfano and S. L. Shapiro
Bayside Research Center, GTE Laboratories, Bayside, New York 11360
(Received 20 January 1971)

The lifetime of the 1086-cm^{-1} optical phonon in calcite is measured directly to be 8.5 ± 2 psec at 297°K and 19.1 ± 4 psec at 100°K by using a picosecond laser beam to create the phonons by stimulated Raman scattering, and then observing Raman scattering off the phonons at various delay times with a weaker picosecond beam at another frequency.

Despite the importance and great interest in the temporal behavior of an optical phonon in solid-state physics and nonlinear optics, the optical-phonon lifetime has never been measured directly. In the past the lifetime has been deduced from the linewidth of spontaneous Raman scattering. This lifetime is typically $\sim 10^{-11}$ sec, too short to measure directly by conventional means. The advent of a mode-locked laser with resolution on a picosecond scale makes such a measurement possible. This paper reports the first direct measurement[1] of an optical-phonon lifetime in a crystal. A calcite crystal has been chosen for this experiment.

In the experiment a high-power picosecond laser beam operating at a wavelength of 1.06 μm creates the optical phonons in calcite by stimulated Raman scattering (SRS). A second, but much weaker, picosecond laser beam operating at a wavelength of 0.53 μm, acting as a probe, travels along a variable optical delay path and undergoes Raman scattering off the created pho-

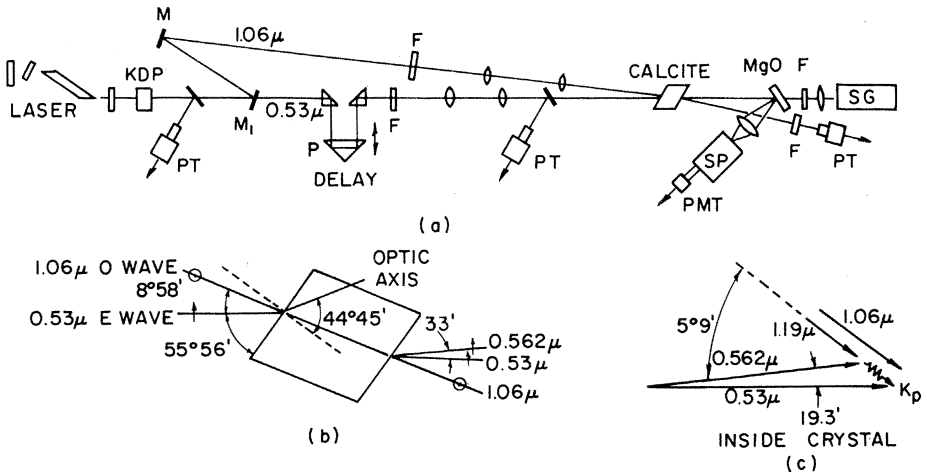

FIG. 1. (a) Schematic of the experimental appratus, (b) the experimental angles for the probe and exciting laser beams outside the calcite, and (c) the noncollinear phase matching inside the calcite.

nons. Such probe scattering off created phonons in calcite has been previously demonstrated,[2] and collisional de-excitation of vibrational levels in hydrogen gas[3] of the order of 10^{-5} sec and acoustic-phonon lifetimes in liquids[4] of the order of 10^{-7} sec have been measured previously by probe techniques. The decay rate of the optical-phonon population is obtained by measuring the intensity of the Raman light produced by the probe as a function of delay between the laser and probe pulses.

The experimental arrangement is shown in Fig. 1(a). The Nd-glass mode-locked laser is described in earlier papers[5] and emits about 50 pulses of $\sim 5\times10^{9}$ W peak power. A fraction of the beam is converted to second harmonic with a peak power of $\sim 2\times10^{8}$ W. The total bursts of radiation for the fundamental and harmonic are 6 and 4 psec, respectively, as measured by two-photon fluorescence.[6] A dielectric mirror (M_1) reflects 99.9% at 1.06 μm and transmits 90% at 0.53 μm. The 1.06-μm beam is collimated to 1 mm in diameter over the sample length of 3 cm and is polarized as an ordinary wave. The 0.53-μm beam is collimated to 4 mm in diameter and traverses the crystal as an extraordinary wave. Figures 1(b) and 1(c) show the experimental angles for Stokes phase matching of the probe beam to the phonons generated by the 1.06-μm beam and also having the ray direction (Poynting vector) of the probe beam collinear with the propagation direction of the phonons and 1.06-μm beams. These conditions can be satisfied in calcite because of its large birefringence. A variable time delay is introduced between the 1.06- and 0.53-μm beams by the movable prism P. The time of coincidence between the probe beam and the exciting beam is found by using the optical Kerr-effect gate[7] of a 1-cm sample of CS_2.[8] Cooled nitrogen gas is used to obtain a temperature of 100°K.

The condensing system for the 1.06-μm beam is carefully adjusted so that no crystal damage occurs. This adjustment is of critical importance to the success of the experiment. Occasionally the crystal is damaged, but when this occurs, the data for the entire run are rejected. Only one of six crystals we tried had a high damage threshold. This crystal—type $B+$ quality—is used for all the experimental data at room temperature. However, at low temperatures many crystals had high damage thresholds.

Self-focusing is observed in the calcite over the last 2 cm. SRS is observed at 1.19 μm with a conversion efficiency of $\geq 1\%$. The Raman pulse widths are estimated from transient Raman-gain equations[9] to be ≤ 2.7 psec. The Raman pulse widths could be shorter because approximately the first ten laser pulses of the train produce SRS,[10] and these pulses are the shortest pulses in time.[11] Therefore, the optical phonons are created in a time less than 2.7 psec. The 0.53-μm light scatters off the phonons and produces probe Stokes light at 0.562 μm with a conversion efficiency of $\cong 0.1\%$. The coherence length[12] for the probe and probe Stokes light is $\sim$11 cm, and the coherence length between the 1.06- and 0.53-μm pulses is ~ 9.3 cm. Therefore, the distance between the 1.06- and 0.53-μm pulses remains constant throughout the sample.

The presence of optical phonons is indicated by the Stokes Raman-scattered probe light at a

wavelength of 0.562 μm which strikes an MgO plate and is imaged on the slit of a $\frac{1}{2}$-m Jarrell-Ash spectrometer. The light is detected by an RCA 7265 photomultiplier. Typically 25 shots are taken at each delay position, and the intensity of the 0.562-μm light is normalized by dividing by the intensity of the 0.53-μm probe beam and 1.19-μm beam. Only about seven shots at each position are analyzed as a datum point—they are chosen on a basis of nearly the same laser intensity and "perfect" mode-locked train as displayed on a Tektronix 519 scope. The 1.06-, 1.19-, 0.53-, and 0.562-μm beams are displayed coincidently on a Tektronix 555 scope. The intensity of the 0.562-μm light is found to be linear with respect to the 1.19-μm intensity.

The following experimental procedures are used to insure that the Raman probe light arises from the created phonons: (1) At room temperature Raman spectra occur at 0.562 μm in a 100-cm^{-1} wide band and appear only when the 1.06-μm beam is present and coincident within ~40 psec with the 0.53-μm light beam. (2) The 0.562-μm light disappears when the 0.53-μm beam is not present. (3) The intensity of the 0.562-μm light depends critically on the orientation of the calcite crystal—the intensity decreases with a full width at half-maximum of 0.6° from the phase-matching angle at room temperature. (4) The 0.562-μm radiation is emitted from the calcite crystal at an angle of 28′ from the propagation direction of the 5300-Å radiation which is in good agreement with calculation.

We have completed the discussion of the necessary experimental procedures and now proceed to the crux of the paper—the optical-phonon lifetime which is obtained from the curve displayed in Fig. 2. Figure 2 shows the best individual runs. The intensity profile of the tail of the curves in Fig. 2 is exponential. It represents a convolution of the exponentially decaying phonon-density profile and the probe laser pulse. The lifetime is obtained from these tails for times much greater than the pulse width of the laser. The curves in Fig. 2 are exponential for ten pulse widths of the probe beam. As long as the phonons decay exponentially, convolution calculations show that the shape of the tail[13] is not altered by the shape of the laser pulses.[14] The best fit to the experimental tail in Fig. 2 is found for the decay rate of 19.1 ± 4 psec at 100°K and 8.5 ± 2 psec at 297°K. At 100°K the average lifetime measured for seven runs is 22 ± 4 psec.

Spontaneous Raman-linewidth measurements[15]

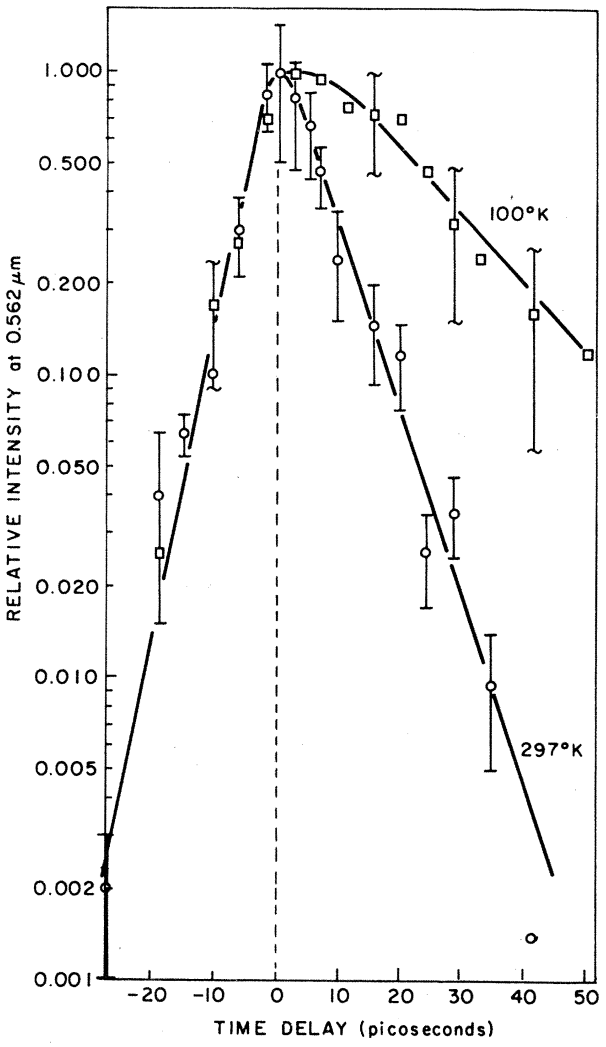

FIG. 2. Normalized Stokes Raman-scattered probe intensity versus delay time between 1.06- and 0.53-μm beams.

indicate a phonon lifetime at room temperature of ≅3.6-4.8 psec and a lifetime of ≅7.7 psec at 100°K. These results are not within our experimental error. The question arises, why should there be a disparity between the direct lifetime measurement and the spontaneous measurement? We offer two possible explanations for the difference. First, decay rates may differ for coherent phonons and thermal phonons.[16] The coherent phonons created by SRS have a state characterized by frequency $\omega_p = 1086\ cm^{-1}$ and wave number $k \cong 0.11 \times 10^5\ cm^{-1}$, and within an angle of 10^{-2} rad. The population of coherent phonons in the same state (element of phase space) is about 10^6 times greater than the thermal background at room temperature and 10^9 times great-

er at 100°K. The relative number of thermal phonons available to scatter with the created phonons is far less than for a thermal distribution of phonons in this state. If the decay mechanism involves interaction with thermal phonons, these coherent phonons will live longer in this state because the thermal phonon background cannot thermalize the large flux of coherent phonons. As evidence supporting this hypothesis, we note that not only is our measurement at room temperature in closer agreement with the decay time obtained from the spontaneous Raman linewidth near liquid-nitrogen temperature[15] (77°K), but also the measurement at 100°K is closer to the spontaneous linewidth measurement of 13.4 ± 4 psec at 4°K. Also, besides thermal saturation effects the decay rate of intense coherent phonons may be influenced by mutual interactions[17] (increasing the lifetime) and parametric-generation decay[18] processes (decreasing the lifetime).

A second explanation for the disparity between the lifetime measurements is that thermal and coherent phonons are located at different points on the optical-phonon branch and thus may have intrinsically different lifetimes.[19] Spontaneous Raman measurements at 90° to the incident beam of wavelength 6328 Å propagating along the c axis determine the linewidth for a phonon with momentum $k_p = 2.3 \times 10^5$ cm^{-1} whereas the direct technique detects a phonon of $k_p = 1.1 \times 10^4$ cm^{-1} propagating at a different angle in the crystal. Since the dispersion curve in calcite is incompletely known,[20] it is impossible to estimate the decay rate for these two different phonons.

In conclusion the first direct measurements of the optical-phonon lifetime show that the optical-phonon lifetime in calcite at both room temperature and at 100°K is considerably longer than that deduced previously from spontaneous measurements.

We thank Dr. A. Lempicki for helpful discussions and for his interest and encouragement during all phases of this experiment, and S. Hussain for technical assistance.

---

[1]R. R. Alfano, Bull. Amer. Phys. Soc. 15, 1324 (1970); R. R. Alfano and S. L. Shapiro, Bull. Amer. Phys. Soc. 16, 53 (1971).

[2]J. A. Giordmaine and W. Kaiser, Phys. Rev. 144, 676 (1966).

[3]F. DeMartini and J. Ducuing, Phys. Rev. Lett. 17, 117 (1966).

[4]W. Heinicke, G. Winterling, and K. Dransfeld, Phys. Rev. Lett. 22, 170 (1969).

[5]R. R. Alfano and S. L. Shapiro, Phys. Rev. Lett. 24, 584, 592, 1217 (1970).

[6]We conservatively choose the total burst of radiation as the pulse width instead of the sharp correlation peak of the two-photon fluorescence pattern which is 2 psec full width at half-maximum for the fundamental; see, for example, S. L. Shapiro and M. A. Duguay, Phys. Lett. 28A, 698 (1969).

[7]M. A. Duguay and J. W. Hansen, Appl. Phys. Lett. 15, 192 (1969).

[8]The intensity of the probe beam versus the delay time between the 1.06- and 0.53-μm beams is a symmetric curve of FWHM ~8 psec, which is approximately the convolution of the 6-psec pulse width of the 1.06-μm beam, 4-psec pulse width of the 0.53-μm beam, and 2-psec Kerr relaxation time of CS_2. This overestimates the prompt curve which is the convolution of the Raman light, of pulse width <2.7 psec, and the effective pulse width of the probe laser off the created phonons, <4 psec.

[9]R. L. Carman, F. Shimizu, C. S. Wang, and N. Bloembergen, Phys. Rev. A 2, 60 (1970).

[10]M. J. Colles, Opt. Commun. 1, 169 (1969); R. L. Carman, M. E. Mack, F. Shimizu, and N. Bloembergen, Phys. Rev. Lett. 23, 1327 (1969); R. R. Alfano and S. L. Shapiro, Phys. Rev. A 2, 2376 (1970).

[11]W. H. Glenn and M. J. Brienza, Appl. Phys. Lett. 10, 221 (1967).

[12]The coherence length $l_c = \tau_p \bar{v}_g / 2\Delta v_g$ for two pulses is defined to be the distance for which two pulses stay spatially coincident by less than a half-pulse width; τ_p is the pulse width, $\bar{v}_g$ is the average group velocity, and Δv_g is the difference in group velocities. The Raman coherence length of 3.0 cm for calcite stated by Colles (Ref. 10) is for ~1 psec pulses. A pulse width of 4 psec is used to compute l_c in this paper.

[13]The convolution of an exponential phonon decay (τ_p) with a Gaussian-shaped laser pulse (full width T_L at half-maximum) rapidly assumes the exponential decay τ_p with an error of ≤ 1 % for $\tau_p \geq T_L$ for $t > T_L$. With an exponential-shaped laser pulse the convolution rapidly assumes the exponential decay τ_p with an error ≤ 10 % for $\tau_p \geq T_L$ for $t > T_L$. For both the lifetimes measured in this paper the error is <1 % due to deconvolution. The precision of the results is not altered for the conservative pulse widths we have chosen (see Ref. 6).

[14]The rise of the intensity curve in Fig. 2 could be fitted by the convolution of the probe laser, the phonons, and the SRS sharpened laser pulse.

[15]K. Park, Phys. Lett. 22, 39 (1966). The linewidth and corresponding calculated lifetime assuming a Lorentzian shape are $\Delta\nu_{300°K} \cong 1.1 \pm 0.12$ cm^{-1}, $\tau_{300°K} \cong 4.8 \pm 0.5$ psec; $\Delta\nu_{100°K} \cong 0.69 \pm 0.12$ cm^{-1}, $\tau_{100°K} \cong 7.7 \pm 1.4$ psec; and $\Delta\nu_{10°K} \cong 0.4 \pm 0.12$ cm^{-1}, $\tau_{10°K} \cong 13.4 \pm 4$ psec. However, the linewidths are in slight disagreement with later reported values by K. Park, Phys. Lett. 25A, 490 (1967), of $\Delta\nu_{300°K} \simeq 1.5$ cm^{-1}, $\tau_{300°K} \simeq 3.6$ psec, $\Delta\nu_{100°K} \cong 0.69$ cm^{-1}, $\tau_{100°K} \cong 7.7$ psec; and $\Delta\nu_{10°K} \simeq 0.5$ cm^{-1}, $\tau = 10.7$ psec (no error bar given).

[16]The discrepancy between the lifetimes may be re-

lated to the depopulation (T_1) and dephasing (T_2) lifetimes since these may be different for thermal and coherent phonons. Alternatively the two measuring techniques may weight differently the relative contributions of T_1 and T_2. The relevance of T_1 and T_2 to the experiment was pointed out by Dr. A. Lempicki.

[17]S. Simons, Proc. Phys. Soc., London 82, 401 (1963).
[18]R. Orbach, Phys. Rev. Lett. 16, 15 (1966).
[19]See, for example, E. R. Cowley and R. A. Cowley, Proc. Roy. Soc., Ser. A 287, 259 (1965); W. J. L. Buyers and R. A. Cowley, Phys. Rev. 180, 755 (1969).
[20]E. R. Cowley, private communication.

d-Band Difficulties in the $\vec{k}\cdot\vec{p}$ Method*

T. J. Kuebbing, K. Schwarz, S. B. Trickey, and J. B. Conklin, Jr.
Quantum Theory Project, Department of Physics and Astronomy, University of Florida, Gainesville, Florida 32601

(Received 24 March 1971)

The $\vec{k}\cdot\vec{p}$-APW (augmented-plane-wave) method (extrapolation of energy bands throughout the irreducible wedge of the first Brillouin zone from a set of APW basis states at one point in the wedge) has been applied to TiC. Very poor results are obtained in comparison to those found for PbTe, the material most studied to date using the method. The difficulty appears to be associated with the d bands in TiC and possibly with the sparseness of states at Γ for certain rather large energy ranges.

In a series of papers[1-6] appearing during the last half-decade, Pratt and co-workers have reported the calculation of energy bands, interband matrix elements of momentum, vacancy-state properties, and optical properties of PbTe. All of this work has as its foundation the $\vec{k}\cdot\vec{p}$-APW (augmented plane wave) method, in which the APW[7] solutions $w_{n\vec{k}}(\vec{r})$ to the one-electron Shcrödinger equation (with local exchange[8]) at $\vec{k}=0$ (or some other point $\vec{k}_0$ of high symmetry) are used to form the trial wave function

$$\Psi_{n\vec{k}}(\vec{r})=\sum_j \beta_{nj}(\vec{k})\exp(i\vec{k}\cdot\vec{r})w_{j\vec{k}_0}(\vec{r}). \quad (1)$$

This wave function then yields the customary $\vec{k}\cdot\vec{p}$ secular equation,

$$\det\{2(\vec{k}-\vec{k}_0)\cdot\langle w_{j\vec{k}_0}|\vec{p}|w_{i\vec{k}_0}\rangle - \delta_{ji}[\epsilon_n(\vec{k})-\epsilon_i(k_0)-(\vec{k}-\vec{k}_0)^2]\}=0, \quad (2)$$

when used in the ordinary Rayleigh-Ritz variational principle. It is straightforward to include relativistic corrections and obtain a generalization of (2); the reported work on PbTe has in fact incorporated such corrections.

Because of the wide range of successful applications of the $\vec{k}\cdot\vec{p}$-APW method to PbTe, we began an effort to develop independent computer programs and make tests of the method on a variety of compounds. It was hoped that a rapid, economical, and widely applicable method for extrapolating energy bands from the APW would result. To this end we selected the NaCl structure (for checking against nonrelativistic PbTe results, and for application to TiC, a compound of independent interest to some of us), and developed the codes necessary for computing the matrix element of momentum which appears in (2), and for subsequently solving (2). Insofar as we are able to ascertain, both the structure of our calculational procedure and some of the numerical methods employed are rather different from those of Pratt *et al.* However, we defer a discussion of these technical points to a forthcoming publication on our techniques.

One sensitive test of the computer code is the calculation of the energy bands for the empty lattice. Using the structure elements, lattice spacing ($a=8.1606$ a.u.), and APW sphere radii appropriate to TiC, we computed energy bands for a potential which vanished everywhere. Included in our basis set for the empty lattice test were symmetrized plane waves with reciprocal lattice vectors of squared magnitude up to and including $32\pi^2/a^2$. Matrix elements of $\vec{p}$ between plane waves belonging to different wave vectors should vanish identically; the magnitude of the calculated values was never in excess of 6×10^{-5} a.u. and was commonly two orders of magnitude smaller. The energy bands were in agreement with the exact analytic results to within 10^{-6} Ry, which is a reasonable limit on our overall numerical accuracy. (The coding is in FORTRAN IV, double precision, using an IBM 360/65. The